CHAPTER III FORMULATION OF REINFORCED SOIL SYSTEM

3.1 GENERAL

The aim of the present research work is to present a realistic and simplified numerical method for the analysis and design of real reinforced soil structures. The word "simplified" here implies to the less assumptions made while idealizing a real complex reinforced structures, so that the prediction is close to the performance of the structure after it is erected. Conventional methods of analysis and design of slope stability problems and retaining walls are applied to the complex reinforced soil structures where a lot of assumptions are made before commencing the computation, e.g. computation of factor of safety, reinforcement force distribution, reinforcement soil interface friction, etc., thus, all most all the reinforced structures are over designed (Yako et al, 1987). Unlike these conventional analyses and design methods, the numerical methodology presented in this chapter can compute such variables without making any assumptions before commencing the computation, i.e., the methodology can compute all the variables simultaneously.

This chapter starts with some review on the essence of plasticity theories, then advances to summarization of the rigid plastic finite element method and finally, a new formulation of the reinforced soil system is derived and incorporated into the rigid plastic finite element method (RPFEM). The formulation of the mechanism of a reinforced soil system, derived at the limit state of soil mass is equally applicable to initial loading stage. Thus, the formulation is illustrated by incorporating into the linear elastic finite element method (LEFEM). The applicability of the methodology is illustrated through some typical reinforced soil problems in the next chapter.

3.2 ESSENCE OF *RPFEM* IN SOIL STRUCTURES

In this section, the existing theoretical basis of upper bound theorem for rigid plastic material is briefly discussed and gradually a new formulation is presented in the context of reinforced soil structure. The detailed formulation on RPFEM can be referred to Tamura et al. (1984, 1987), Asaoka et al. (1990, 1992, 1993, 1994) and Kodaka (1993).

3.2.1 Basics on Plasticity Theories

Before we proceed to formulate the soil structure at limit state, some important terms and postulates are summarized. At the outset, a relation between the stresses and the plastic strains is presented based on the Drucker's fundamental quasi-thermo dynamic postulate, also called the Drucker's stability postulate.

***Drucker's Stability Postulate*:**

The Drucker's fundamental quasi-thermo dynamic postulate (Drucker, 1951) states that:

a. If σ_{ij} is a state of stress on the yield surface in which non-vanishing plastic strain rates $\dot{e}_{ij}^{p}$ occur

$$\left(s_{ij} - s_{ij}^{a}\right)\cdot\dot{e}_{ij}^{p} \geq 0 \qquad ...(3.1)$$

for all "allowable" states of stress s_{ij}^{a}. Koiter (1962) has geometrically explained implications of Drucker's principle of maximum work (Eq. 3.1). Koiter (1962) stated that no change in the plastic strains, $\dot{e}_{ij}^{p}$, of an element is assumed to occur if the stress, s_{ij}, point lies in a elastic domain; such a state of stress is called "safe" s_{ij}^{s}. Increments of the plastic strains, $\dot{e}_{ij}^{p}$, can only occur if the stress point is at the boundary of the elastic domain, which is called as yield limit, or in geometric terms the yield surface. A state of stress that is either in the elastic domain or on the yield surface is called "allowable" s_{ij}^{a}. He further stated that the aforesaid condition (Eq. 3.1) has very significant implications and restriction on the shape of yield surface. Thus, Drucker's fundamental postulate entails the following consequences:

b. If ds_{ij} are the stress rates corresponding to the plastic strain rates $\dot{e}_{ij}^{p}$, then the strain rate vector, $\dot{e}_{ij}^{p}$ is normal to the yield surface (Fig. 3.1). Mathematically-

$$ds_{ij}\cdot\dot{e}_{ij}^{p} = 0 \qquad ...(3.2)$$

c. The yield surface is convex.

It should be noted that Drucker's fundamental postulate has consequences only for the plastic strain rates; no statement can be made on the total plastic strains unless the entire history of the element has been specified.

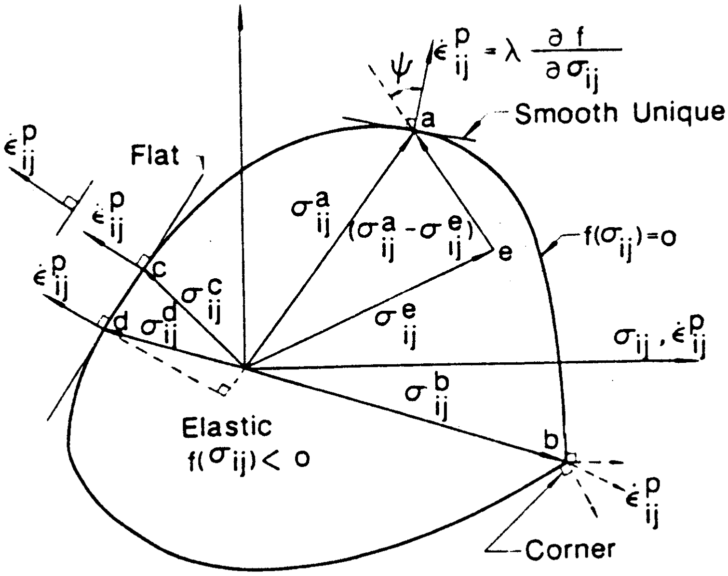

Figure 3.1 Graphical representation of yield surface (*Chen and Liu, 1991*)

Rate of Plastic Energy Dissipation

The rate of plastic energy dissipation per unit volume (i.e. specific volume) is:

$$D(\dot{e}_{ij}^{p}) = s_{ij} \cdot \dot{e}_{ij}^{p} \qquad \text{...(3.3)}$$

where s_{ij} is the state of stress on the yield surface in which the non-vanishing plastic strain rates $\dot{e}_{ij}^{p}$ occur. It is a single valued function of the plastic strain rates that increases proportionally with the increase of the plastic strain rates. The properties of the rate of plastic energy dissipation may be summarized as follows:

a. Since s_{ij} is independent of the magnitude of $\dot{e}_{ij}^{p}$, then $D(\dot{e}_{ij}^{p})$ is linear with $\dot{e}_{ij}^{p}$.

b. The differential of *D*, is $dD = s_{ij}.d\dot{e}_{ij}^{p} + ds_{ij}.\ \dot{e}_{ij}^{p}$ and $ds_{ij}.\dot{e}_{ij}^{p}$ is zero based on the normality rule. Thus, $dD = s_{ij}.d\dot{e}_{ij}^{p}$.

c. $D(\dot{e}_{ij}^{p})$ is convex in $\dot{e}_{ij}^{p}$ if it is continuously differentiable, e.g. $D(\dot{e}_{ij}^{p})$. (Fig. 3.2).

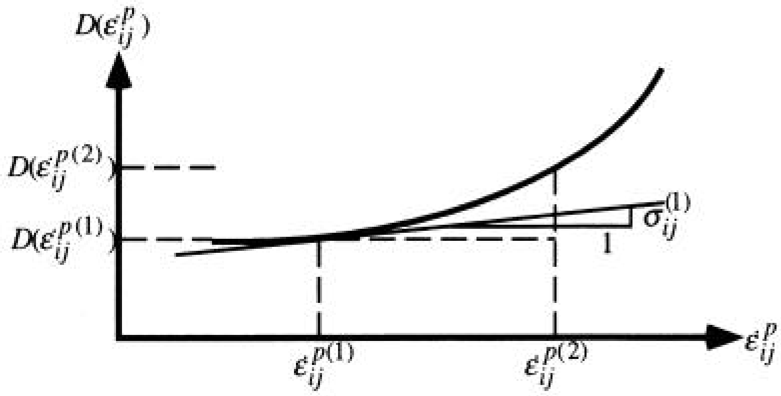

Figure 3.2 Graphical explanation of the convexity and continuously differentiability of the energy function (*Kodaka*, 1993)

d. Though non-vanishing plastic strain rate, $\dot{e}_{ij}^{p}$, occurs, Mises material exhibits additional special feature with respect to the rate of volumetric strain at limit state.

Yield function for Mises material, $f(s_{ij}) = \frac{1}{2}(s_{ij}\, s_{ij} \; - \; s_{0}^{2})$ ...(3.4)

where, s_{0} is Mises constant. The corresponding plastic strain rate, $\dot{e}_{ij}^{p}$, can be derived following the normality rule:

$$\dot{e}_{ij}^{p} = l\,\frac{\partial f}{\partial s_{ij}} = l\,S_{ij} \qquad \text{...(3.5)}$$

here, $l = \frac{\bar{\dot{e}}}{s_{0}}$ is plastic multiplier, and $\bar{\dot{e}} = \sqrt{\dot{e}_{ij}\dot{e}_{ij}}$ is equivalent plastic strain rate. Eq. (3.5) gives the plastic volumetric strain rate, $\dot{e}_{v}^{p}$, as follows:

Volumetric plastic strain: $\dot{e}_{v}^{p} = \dot{e}_{ii}^{p} = 0$ ...(3.6)

Therefore, when the plastic flow of Mises material is discussed, the plastic strain rate with non-vanishing volumetric component cannot be employed for the computation of plastic energy dissipation. The plastic energy dissipation rate, $D(\dot{e}_{ij}^{p})$ for Mises material is given by

$$D(\dot{e}_{ij}^{p}) = s_{0}\,\bar{\dot{e}} \qquad \text{...(3.7)}$$

Likewise some constraint conditions should be imposed on the plastic flow, $\dot{e}_{ij}^{p}$, depending on the type of yield function adopted in the analysis.

***Compatibility Condition*:**

The plastic strain rate, $\dot{e}_{ij}^{p}$, can be derived from the velocity, $\dot{u}_i$, by means of the following formula called compatibility relation for small deformation theory:

$$\dot{e}_{ij}^{p} = \frac{1}{2}\left(\dot{u}_{i,j} + \dot{u}_{j,i}\right) \quad in \;\; V \qquad ...(3.8)$$

where a comma preceding a subscript *i* denotes partial differentiation with respect to the coordinate X_i. The velocity satisfies the boundary conditions on S_u

$$\dot{u}_i = \dot{u}_{i0} \qquad ...(3.9)$$

***Load Factor*:**

Safety factor/load factor, r corresponding to a given system of external loads X_i, T_i (considering X_i be the body force distribution in V and T_i be the traction on the traction boundary S_σ) is defined as the positive multiplier with the property that the loads rX_i and rT_i constitute a limit load system. In certain cases, the pair (X_i, T_i) implies the external forces of unit magnitude.

***Limiting Equilibrium State*:**

The limit state is defined as the state of equilibrium of forces at which all the soil elements have reached the failure state and their associated plastic strain rates satisfy compatibility conditions with continuous, non-zero velocity field. At limit state, thus, a rigid plastic material (e.g., purely cohesive clay) exhibits following characteristics:

(a) The plastic strain rate, $\dot{e}_{ij}^{p}$, of soil element is indeterminate at the failure state of soil.

(b) The stress, s_{ij}^{*}, on the yield surface, which is derived from, $\dot{e}_{ij}^{p}$, through the associated flow rule, forms a equilibrium state with the external forces $(r^{*}X_i, r^{*}T_i)$.

(c) The volumetric plastic strain rate is zero. ($\dot{e}_{ij}^{p}$ =0).

***Upper Bound Theorem*:**

Consider that the X_i, T_i are the given external forces and a new subset $Kp\,(\grave{I}\;K)$ may be introduced as follows:

$$K_p = \left\{ \left(\dot{e}_{ij}^{p}, \dot{u}_i\right) \in K \middle| \int_V X_i \dot{u}_i \; dV + \int_{S_s} T_i \dot{u}_i \; dS \geq 0 \right\} \qquad ...(3.10)$$

For any given kinematically admissible strain rate and velocity fields, $(\dot{e}_{ij}^{p}, \dot{u}_i) \in K$, the load factor, r, may be defined as follows:

$$r = \frac{\int_V D(\dot{e}_{ij}^{p})\ dV}{\int_V X_i \dot{u}_i\ dV + \int_{S_s} T_i \dot{u}_i\ dS} \qquad ...(3.11)$$

The upper bound theorem states

$$r \geq r^{*} \qquad ...(3.12)$$

where r^{*} is the load factor at the limit state and this condition introduces the minimization problem of r with respect to $\dot{u}_i$.

As mentioned before, $D(\dot{e}_{ij}^{p})$ is linear with $\dot{e}_{ij}^{p}$ (or equivalently $\dot{u}_i$.) and other terms in the denominator are also linear with $\dot{u}_i$, therefore, problem of minimization of r with respect to $\dot{u}_i$ can be equivalently replaced by the following problem. In this case, the global shape of spatial distribution of external forces is assumed to be of unit magnitude. There exist an additional constraint condition of no volume change at limit state of soil. Such that the problem reduces to:

Problem A

$$Minimize \int_V D(\dot{u}_i)\ dV \qquad ...(3.13)$$

$$Subject\ to\ \int_V X_i \dot{u}_i\ dV + \int_{S_s} T_i \dot{u}_i\ dS = 0 \qquad and\ \ \dot{e}_{kk} = 0 \qquad ...(3.14)$$

3.2.2 Rigid Plastic Finite Element Method (*RPFEM*)

The detailed procedure for the minimization of the internal plastic energy dissipation rate, $D(\dot{u}_i)$, with respect to kinematically admissible velocity field which reduces the upper bound theorem in plasticity to the equilibrium equation of forces at limit state was clearly explained by Tamura et al.(1984) using the finite element discretization technique. In this section, referring Tamura et al.(1984), the limiting equilibrium equations are illustrated through finite element discretized notations. This finite element discretization technique has been called the rigid plastic finite element method (RPFEM) which was pioneered by Tamura et al.(1984) in the field of geotechnical engineering. The following Problem B equivalently replaces using FE discretized notations, the earlier Problem A:

Problem B

$$\begin{aligned}&Minimize \int_V D(\dot{\boldsymbol{u}})\ dV \\ &Subject\ to \begin{cases}\boldsymbol{F}^T\dot{\boldsymbol{u}} = 1 \\ L\dot{\boldsymbol{u}} = \mathbf{0}\end{cases}\end{aligned} \qquad ...(3.15)$$

in which $\boldsymbol{F}$ is the vector of all nodal forces expressing the shape of external forces of an unit magnitude. L is the matrix defined such as, where $L\dot{\boldsymbol{u}} = \dot{\boldsymbol{v}}$ is the vector of all nodal velocities, while $\dot{\boldsymbol{v}}$ is the rate of volume changes in all elements. The constraint condition, $\boldsymbol{F}^T\dot{\boldsymbol{u}} = 1$, in Eq.(3.15) defines the provisional norms of velocity vector and the other one, $L\dot{\boldsymbol{u}} = \mathbf{0}$ indicates that no rates of volume change should occur at all elements in the limit state, which reflects the non-dilatant characteristics of the Mises material described later.

The problem defined above falls in the category of a convex programming problem where a local minimum is the global minimum. Introducing the Lagrange multipliers l & m and finally minimizing the following functional have applied the limit analysis based on the upper bound theorem,

$$j\,(\dot{\boldsymbol{u}}, l, m) = \int_V D(\dot{\boldsymbol{u}})\,dV + l^T\left(\boldsymbol{L}\dot{\boldsymbol{u}} - \mathbf{0}\right) + m\left(\boldsymbol{F}^T\dot{\boldsymbol{u}} - \mathbf{1}\right) \qquad ...(3.16)$$

As $D(\dot{\boldsymbol{u}})$ is the convex function of $\dot{\boldsymbol{u}}$, a stationary condition of J gives the global minimum of J. Thus, the finite element formulation of the limit state problems is considered as a problem of finding out the stationary condition for the above functional.

The stationary condition for the above functional corresponding to any virtual variations $d\dot{\boldsymbol{u}}$, dl and dm can be given as follows:

$$\int_V dD(\dot{\boldsymbol{u}})\ dV + l^{?} Ld\dot{\boldsymbol{u}} + m\boldsymbol{F}^{?} d\dot{\boldsymbol{u}} = 0 \qquad ...(3.17)$$

$$dl^T\ \ L\dot{\boldsymbol{u}} = 0 \qquad ...(3.18)$$

$$dm\left(\boldsymbol{F}^T\dot{\boldsymbol{u}} - 1\right) = 0 \qquad ...(3.19)$$

Since, $dD = s_{ij}^T\, d\dot{e}_{ij}^p = s^T\,(B\, d\,\dot{\boldsymbol{u}}^T)$, then, Eq. (3.17) can be written as:

$$\int_V (s^T B)\ dV + l^{?} Ld\dot{\boldsymbol{u}} + m\boldsymbol{F}^{?} d\dot{\boldsymbol{u}} = 0 \qquad ...(3.20)$$

In the above equations (Eqs. 3.18~20) $d\dot{\boldsymbol{u}}$, dl and dm can be completely arbitrary provided they are continuous. Therefore, the following equilibrium equations are obtained by eliminating these terms:

Problem C

$$\int_V B^T \boldsymbol{s}\, dV + L^T l + m\boldsymbol{F} = \boldsymbol{0} \qquad \text{...(3.21)}$$

$$L\dot{\boldsymbol{u}} = 0 \qquad \text{...(3.22)}$$

$$\boldsymbol{F}^T \dot{\boldsymbol{u}} = 1 \qquad \text{...(3.23)}$$

in which $\boldsymbol{s}$ denotes deviator stress vector while m is interpreted as load factor of external forces and l as the indeterminate isotropic stress in $\boldsymbol{V}$.

These equilibrium equations can be directly obtained after minimizing the function J with respect to the velocity field, $\dot{\boldsymbol{u}}$, and Lagrange multipliers, l and m, respectively.

Problem D

Often some relations among velocity components at the displacement boundary are assigned a priori such as in the case of loading through the rigid plate. For example, consider the following problem:

$$\text{Minimize } \int_V D(\dot{\boldsymbol{u}})\; dV$$
$$\text{Subject to } \begin{cases} C\dot{\boldsymbol{u}} = \boldsymbol{a} \\ L\,\dot{\boldsymbol{u}} = \boldsymbol{0} \end{cases} \qquad \text{...(3.24)}$$

in which $\boldsymbol{a}$ is the prescribed vector and Eq. (3.24) is a linear constraint for $\dot{\boldsymbol{u}}$. The function J can be replaced by a new function, Y, as:

$$j\left(\dot{\boldsymbol{u}}, l, m\right) = \int_V D(\dot{\boldsymbol{u}})\, dV + l^T (\boldsymbol{L}\dot{\boldsymbol{u}} - \boldsymbol{0}) - m^T (\boldsymbol{C}\dot{\boldsymbol{u}} - \boldsymbol{a}) \qquad \text{...(3.25)}$$

in this problem. Hence, following the similar procedure as before, the stationary condition of Y can be derived in the following form:

$$\int_V B^T \boldsymbol{s}\, dV + L^T l = C^T m \qquad \text{...(3.26)}$$

which can be regarded as the equilibrium condition corresponding to each nodes.
Rigid smooth footing case

$$\dot{u}_{v0} = \dot{u}_0 \qquad \text{...(3.27)}$$

Rigid rough footing plate exhibits following conditions:

$$\dot{u}_{v0} = \dot{u}_0 \text{ and } \dot{u}_{h0} = 0 \qquad \text{...(3.28)}$$

3.2.3 Constitutive Relationship of Soils at the Limiting Equilibrium State

Eqs. (3.21)-(3.23) define statically indeterminate limiting equilibrium problems and they are solved with the aid of a constitutive relationship of soils at the limit state. Two types of soil are considered in the present study and both soils are assumed to exhibit non-dilatant characteristics at limit state. Then, they are assumed to follow the Mises type plastic flow at limit state. In this sub-section, the constitutive relationship of soils at limit state are discussed and compared with the well-known Cam-clay model at the critical state.

Yield Function of Soil and Limiting Equilibrium State

Terzaghi (1936) introduced the concept of effective stress and the mathematical relationship between total stress, effective stress and pore pressure. He defined the effective stress, as "*All measurable effects of a change of stress, such as compression, distortion and a change of shearing resistance are due exclusively to changes of effective stress The effective stress* s' *is related to the total stress* (s) *and pore pressure* (u) *by* $s' = s$-u". Thus,

$$s'_{ij} = s_{ij} - u d_{ij} \qquad ...(3.29)$$

where, s'_{ij} = the effective stress,

s_{ij} = the total stress,

u = the pore pressure and

d_{ij} = Kroneckor delta (d_{ij} =1 if i=j, else d_{ij} =0)

Based on Henkel (1960), it can be stated that the volumetric strain is caused by the effective stress components and independent of stress path. The volumetric strain can be mathematically represented as:

$$e_v = e_v(s'_{ij}, s'_{ij0}) \qquad ...(3.30)$$

The total volumetric strain can be separated into two elastic and plastic components, $e_v = e_v^e + e_v^p$. The elastic component of the volumetric strain, i.e. $e_v^e = e_v^e(s'_{ij}, s'_{ij0})$, is reversible.

In the present study soils are assumed to follow the associated flow rule with the following type of yield function in terms of effective stresses:

$$e_v^p = f(s'_{ij}, s'_{ij0}) \qquad ...(3.31)$$

in which the plastic volumetric strain, e_v^p, is considered as a hardening parameter, s'_{ij} represent the current effective stress and $s'_{ij\,0}$ represent initial effective stress which gives reference state from which plastic strain rate begins to be measured, i.e., $\dot{e}_v^p$ =0 when $s'_{ij} = s'_{ij\,0}$.

From Eq. (3.31),

$$d\varepsilon_v^p = df = \frac{\partial f}{\partial \sigma'_{kl}} d\sigma'_{kl} \qquad \text{...(3.32)}$$

The critical state is defined here as the state at which the magnitude of plastic strain increment becomes indeterminate even when no increments of stresses($d\sigma'_{kl}$ =0) are applied. When no increments of stresses are considered, it follows from Eq.(3.32) that

$$\dot{\varepsilon}_v^p = \dot{\varepsilon}_v^e = 0 \qquad \text{at critical state.} \qquad \text{...(3.33)}$$

Note that ($d\varepsilon_{ij}^p = \dot{\varepsilon}_{ij}^p\, dt$ *where dt is a scalar quantity*)

Now, based on the associated flow rule,

$$d\varepsilon_{ij}^p = \lambda \frac{\partial f}{\partial \sigma'_{ij}} \qquad \text{...(3.34)}$$

After some mathematical manipulations of Eq. (3.33~3.34), one gets the plastic multiplier as follows:

$$\lambda = \frac{\dfrac{\partial f}{\partial \sigma'_{kl}} d\sigma'_{kl}}{\dfrac{\partial f}{\partial \sigma'_{mn}} . \delta_{mn}} \qquad \text{...(3.35)}$$

Finally, the plastic strain rate is given by:

$$d\varepsilon_{ij}^p = \frac{\dfrac{\partial f}{\partial \sigma'_{kl}} d\sigma'_{kl}}{\dfrac{\partial f}{\partial \sigma'_{mn}} .\delta_{mn}} \frac{\partial f}{\partial \sigma'_{ij}} \qquad \text{...(3.36)}$$

Thus, based on the normality assumption [Eq. (3.34)], the critical state condition in terms of effective stresses is obtained so that plastic multiplier [Eq. (3.35)] may become indeterminate under no incremental stress condition, that is

$$\frac{\partial f}{\partial \sigma'_{mn}} \delta_{mn} = 0 \qquad \text{...(3.37)}$$

At the critical state, it should also be noted that no rate of volume change should occur, whereas the magnitude of other plastic strain rate components, $\dot{\varepsilon}_{ij}^p$, are still indeterminate [Eq. (3.36)].

In this study, the state of equilibrium of forces at which all the soil elements have reached the critical state is called the limit equilibrium state. Their associated plastic strain rates at limit state should satisfy compatibility conditions with non-zero velocity field.

At the critical state, the stress-strain rate relationship can be written concretely only when yield function is identified. The stress-strain rate relationship is demonstrated through the well-known yield function for the Cam-clay model.

Critical State of Soils in the Perspective of Cam-clay Model

Researchers at Cambridge University derived a very simple theoretical formulation of the critical state of soils during 1960s (e.g., Roscoe et al., 1963). Over the years many researchers have modified the original Cambridge Model called "*Cam-clay Model*" (Roscoe-Burland, 1968; Sekiguchi-Ohta, 1977; etc.). All the theories within the Cam clay family are basically similar. The state boundary surface is taken as a yield surface as well as a plastic potential surface, and the hardening is related to the plastic volumetric strain given by following equation:

$$e_v^p = f = M D \ln \frac{p'}{p'_o} + D h' \qquad ...(3.38)$$

where, f = yield function,

M = material parameter of soil at critical state,

D = dilatancy parameter of soil

p' = σ_m', mean effective stress,

p_o' = mean effective stress at reference state such that (when q=0, p'=p_o')

q = $\sqrt{\frac{3}{2} s_{ij} s_{ij}}$ deviator stress = $\sqrt{\frac{3}{2}} s_o$ (for Mises Material)

h' = effective stress ratio=q/p',

The critical state condition (Eq. 3.37)

$$\frac{\P f}{\P s'_{mn}} d_{mn} = 0 \qquad ...(3.39)$$

After simple manipulations, Eq.(3.38) at the critical state condition reduces to the following simple form:

$$q = M p' \qquad ...(3.40)$$

where M is a critical state parameter. Following the associated flow rule, $de_{ij}^p = l \frac{\P f}{\P s'_{ij}}$, the plastic strain rate de_{ij}^p in Cam-clay model at critical state is as follows:

$$d\varepsilon^p_{ij} = \lambda \left(\frac{D}{p'} \frac{\partial q}{\partial \sigma'_{ij}} \right) \qquad ...(3.41)$$

Differentiating $q = \sqrt{\frac{3}{2} s_{ij} s_{ij}}$, one gets,

$$\frac{\partial q}{\partial \sigma'_{ij}} = \frac{3}{2} \left(\frac{3}{2} s_{ij} s_{ij} \right)^{-\frac{1}{2}} s_{ij} \qquad ...(3.42)$$

Then, $d\varepsilon^p_{ij}$ is simplified as:

$$d\varepsilon^p_{ij} = \lambda \frac{D}{p'} \frac{3}{2} \left(\frac{3}{2} s_{ij} s_{ij} \right)^{-\frac{1}{2}} s_{ij} \qquad ...(3.43)$$

Defining a new term called equivalent plastic strain rate:

$$\bar{\dot{\varepsilon}} = \sqrt{\dot{\varepsilon}_{ij} \dot{\varepsilon}_{ij}} = \sqrt{\frac{3}{2}} \lambda \frac{D}{p'} \qquad ...(3.44)$$

Thus, the plastic multiplier in the Cam-clay model is:

$$\lambda = \frac{\bar{\dot{\varepsilon}}}{\sqrt{\frac{3}{2} \frac{D}{p'}}} \qquad ...(3.45)$$

Substituting Eq.(3.45) in Eq.(3.43) and after some mathematical manipulations, one gets,

$$\dot{\varepsilon}^p_{ij} = \sqrt{\frac{3}{2}} \frac{\bar{\dot{\varepsilon}}}{M} \lambda \frac{1}{p'} s_{ij} \qquad ...(3.46)$$

Thus, the normality rule uniquely determines the direction of plastic strain rate in terms of stresses at the critical state whereas the norm of strain rate is still remains indeterminate. Eq.(3.46) shows that the plastic flow of Cam clay at critical state is absolutely identical to the plastic flow of rigid plastic Mises material, i.e. $d\varepsilon^p_{ij} = \lambda\, s_{ij}$.

The plastic energy dissipation rate in Cam-clay model at critical state can be obtained by substituting Eq.(3.45) in Eq.(3.46) and after some mathematical steps as follows:

$$\begin{aligned} D(\dot{\varepsilon}^p_{ij}) &= d\sigma_{ij}\, \dot{\varepsilon}^p_{ij} \\ &= \sqrt{\frac{2}{3}} M p' \bar{\dot{\varepsilon}} \end{aligned} \qquad ...(3.47)$$

For Mises material, $q = \sqrt{\frac{3}{2}} s_0$, the plastic energy dissipation rate is given by,

$$D(\dot{e}_{ij}^{p}) = s_0 \bar{\dot{e}} \qquad \text{...(3.48)}$$

Cam-clay model at the critical state and Mises material resembles similarity regarding the plastic energy dissipation rate.

Generally, the limiting equilibrium state of saturated soil is solved taking into account of drainage conditions during loading state before reaching the limit state. In the present study, non-dilatant characteristics are assumed at the limit state. Two distinct states are usually discussed, first one is undrained problem and the other, fully drained problem. Most real problems lie in between these two extreme states during loading over saturated soil mass; however, these two states are discussed here for the illustration purposes.

UNDRAINED CONDITION (e.g. *purely cohesive clay*)

In the analysis of undrained problems, no flow of water into or out of any soil element during entire loading procedure is assumed and called as the undrained loading. Because of undrained condition, the soil is assumed to exhibit constant volume throughout the undrained loading procedure. This characteristics provides unique undrained path from the initial stress state to the critical state of the soil element, thus exhibit unique shear strength at failure. When undrained loading for the Cam-clay model is considered, the mean effective stress state at limit state can be determined from the initial effective stress state, and is independent of the boundary conditions for the undrained loading. The mean effective stress state at the limit state for undrained loading is given by:

$$(p')_f = p'_0 \, exp(-L) \,, \quad where \quad L = 1 - \frac{k}{l} \qquad \text{...(3.49)}$$

where l and κ are compression and swelling indices, respectively. In real problems, the soil exhibiting very low permeability is assumed to reach the failure state under undrained condition, therefore the shear strength of the soil, i.e. material constant, is already known before loading procedure is commenced. Such a soil is generally known as "purely cohesive soil".

In Japanese practice, the unconfined compressive strength, c_u, is frequently used in the design and analysis of grounds having such purely cohesive clays. The undrained strength of such clay, c_u, is shown to give following relationship:

$$c_u = \frac{s_1 - s_3}{2} \qquad \text{...(3.50)}$$

in which s_1 and s_3 are the maximum and the minimum principal stresses, respectively. Since deviator stress, q, is $\sqrt{3}c_u$ in the plane strain conditions, the following relationship is derived:

$$\sigma_0 = \sqrt{2}c_u \qquad ...(3.51)$$

FULLY DRAINED CONDITION (*e.g. Sandy soils*)

In the fully drained loading problems, the excess pore pressure distribution at limit state is always assumed dissipated (Du_f=0). Thus, the flow of water in such fully drained (Du_f=0) soil mass can be computed independent of failure mechanism. Such a condition usually observed in the case of soils exhibiting high permeability e.g. sandy soils. In the fully drained problems, therefore, the mean effective stress at critical state is given by:

$$(p')_f = (p)_f - u_s \qquad ...(3.52)$$

when, $$(Du)_f = 0 \qquad ...(3.53)$$

where u_S is the pore pressure distribution at limit state assigned as priori (before loading) and p_f is the mean total stress that should be given by a solution of l in limiting equilibrium equations. Then, Eq.(3.52) should be solved simultaneously with Eqs.(3.21~23), and with constitutive equations at critical state, Eq. (3.43). In this numerical method, the mean effective stress is assumed arbitrarily in the very first step of the iterations and is modified in all the subsequent steps using Eq.(3.52) at the limit state solutions. The limit state reached under fully drained condition has no effect of the initial stress. Thus, the fully drained analysis using aforementioned numerical procedure (Cam-clay model at critical state) requires only one additional material parameter, the critical state parameter, M in addition to the unit weight of soil. Furthermore, the similarity between Cam-clay model at the critical state and Mises material has been demonstrated. The Mises constant, s_0, is considered to exhibit similarity with the critical state parameter, M, in Cam-clay model and the relationship can be written as follows:

$$\sigma_0 = \sqrt{\frac{2}{3}}\, Mp'_f \qquad ...(3.54)$$

In the case of purely cohesive soil, $p'_f(s_0)$ is unique for each soil element before loading procedure as an independent of the boundary conditions. But, in this drained condition, the p'_f is the solution of the boundary value problem because the $p'_f(s_0)$ depends on the p_f as shown earlier in Eq. (3.52). Therefore, the iterative method is required to solve this problem as stated before. It should be noted here that the shear strength in this case are different for each element because the void ratio can be easily changed due to the flow of pore water.

In real problems, especially, when the reinforced soil in sandy soil slopes is considered the fully drained cases are very few whereas almost all the cases are either in dry or in unsaturated conditions where the pore water flow does not exist. The relationship between p'_f and p' in such cases can, therefore, be written as follows:

$$p'_f \;=\; p_f \qquad \text{...(3.55)}$$

In the practical design, the internal friction angle, f, is frequently used. As the relationship between f and M is written as $M=\sqrt{3}\;sin f$ under the plane strain condition, then the Mises constant σ_0 can be expressed as follows:

$$s_0 = \sqrt{2}\;p_f\;sin f \qquad \text{...(3.56)}$$

As far as the unsaturated soil is concerned, the cohesion, *c*, should also be taken into account. Referring both the Drucker-Prager type failure criteria as well as the Mohr's circle envelope, the following relation is obtained for the plane strain condition (Tamura et al., 1987).

$$s_0 = \sqrt{2}\,c\,cos f + \sqrt{2}\;p'_f\;sin f \qquad \text{...(3.57)}$$

It should be noted that Eq. (3.57) is not a yield function but just a failure criteria adopted in this study exactly same as $q=Mp'$. In the case of sandy soil (c=0), Eq. (3.57) reduces to Eq. (3.56) and in the case of f=0, purely cohesive soil, Eq. (3.57) reduces to Eq. (3.51). As the principle of effective stress cannot be discussed concerning the unsaturated soils, therefore, it is not yet known whether the unsaturated soil exhibits the Mises flow at the critical state. However, Mises flow is assumed in the present study it as in the saturated purely cohesive soil.

The structure of sandy soil is; therefore, modeled as an assembly of the inhomogeneous Mises materials where each soil part consists of different σ_0 with respect to corresponding confining pressure, *see* Fig. 3.3. In this case, the limit equilibrium equation is solved iteratively because the Mises constant σ_0 here is a function of the mean effective stress 1 (i.e., p_f') as shown in Eq. (3.57). The iterative procedure is illustrated through the flow chart as shown in Fig. 3.4. Through the flow chart (Fig. 3.4), it can be observed that this problem seems to follow the non-associated flow rule (Tamura et al., 1987), however, the solutions obtained by iterative calculations satisfy the associated flow rule once convergence is achieved.

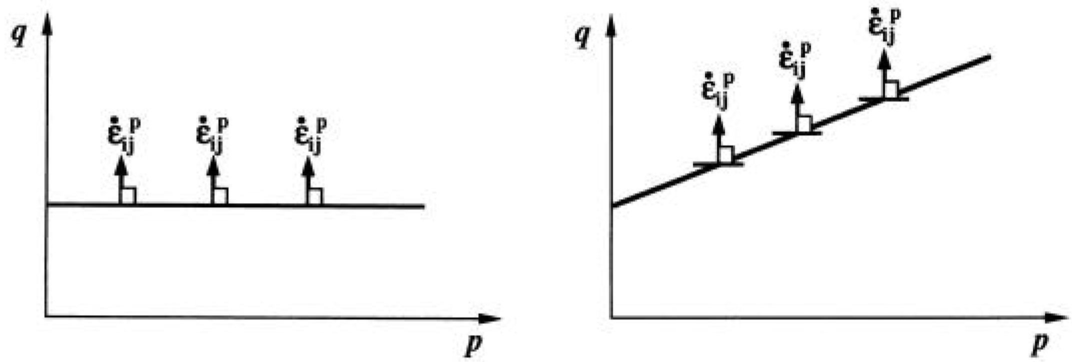

Figure 3.3 Idealization of the frictional (c-ϕ) as an assembly of inhomogeneous Mises materials of varying, σ_O.

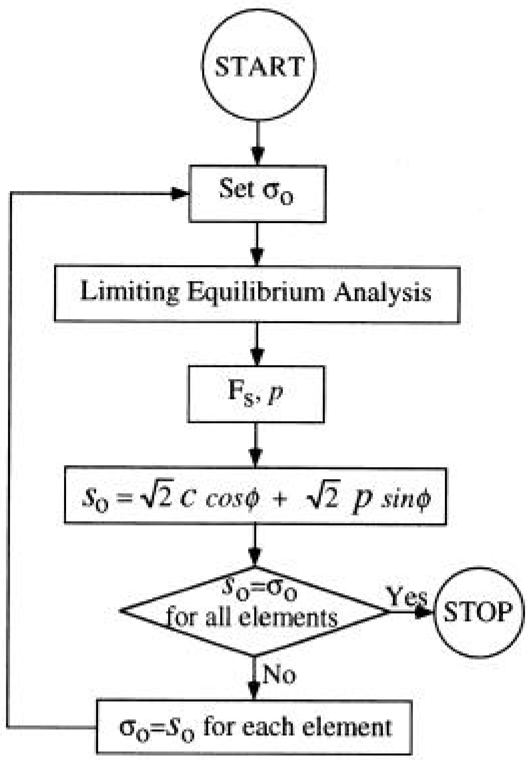

Figure 3.4 Flow Chart adopted for the Numerical Simulations based on RPFEM

3.2.4 Numerical Procedures and Example

Assume that the whole region is in plastic state without unloading. Substituting Eq.(3.5) in to Eq.(3.21) we have the following system of non linear equations for $\dot{\boldsymbol{u}}$, l and m.

$$\left(s_0 \int_V \frac{B^T Q B}{\bar{\dot{e}}} \right) \dot{\boldsymbol{u}} + \boldsymbol{L}^T l = m\boldsymbol{F} \qquad \text{...(3.58)}$$

$$L\dot{\boldsymbol{u}} = 0 \qquad \text{...(3.59)}$$

$$\boldsymbol{F}^T \dot{\boldsymbol{u}} = 1 \qquad \text{...(3.60)}$$

In the above σ_0 is the only one material constant for the analysis. The plastic strain rate calculated by Eq.(3.57) has obviously no volumetric component.

$$\bar{\dot{e}} = \sqrt{\dot{\boldsymbol{u}}^T B^T Q B \dot{\boldsymbol{u}}} \qquad \text{...(3.61)}$$

where ,
$$Q = \begin{bmatrix} 1 & 0 & 0 \\ 0 & 1 & 0 \\ 0 & 0 & \frac{1}{2} \end{bmatrix} \qquad \text{...(3.62)}$$

The equation, Eq.(3.61), can be derived as follows:

$$\begin{aligned} \bar{\dot{e}} &= \sqrt{\dot{e}_{ij}^{p} \dot{e}_{ij}^{p}} = \sqrt{\dot{e}_x \dot{e}_x + \dot{e}_z \dot{e}_z + 2\dot{e}_{xz} \dot{e}_{xz}} \\ &= \sqrt{\dot{e}_x \dot{e}_x + \dot{e}_z \dot{e}_z + 2\dot{g}_{xz} \dot{g}_{xz}} \\ &= \sqrt{\dot{e}^{?} Q \dot{e}} = \sqrt{\dot{\boldsymbol{u}}^{?} B^T Q B \dot{\boldsymbol{u}}} \end{aligned} \qquad \text{...(3.63)}$$

The above set of simultaneous equations, Eqs. (3.58~60) are iteratively solved. Thus, $\dot{\boldsymbol{u}}_{(n)} = \dot{\boldsymbol{u}}_{(n-1)} + aD\dot{\boldsymbol{u}}_{(n-1)}$, $a \geq 0$ in every *n*th step of calculations. The multiplier α is used to control the rate of convergence and generally varies between 0.1 and 1.0 depending on the state of convergence. In all the calculation, the $\Delta\dot{\boldsymbol{u}}_{(n)}$ computed till it practically diminishes to zero i.e. $\dot{\boldsymbol{u}}_{(n)} = \dot{\boldsymbol{u}}_{(n-1)}$.

$$\left(s_0 \int_V \frac{B^T Q B}{\bar{\dot{e}}} \right) (\dot{\boldsymbol{u}} + D\dot{\boldsymbol{u}}) + \boldsymbol{L}^T l - m\boldsymbol{F} = 0 \qquad \text{...(3.64a)}$$

or,

$$\left(s_0 \int_V \frac{B^T QB}{\bar{\dot{e}}}\right)\dot{\boldsymbol{u}} + \boldsymbol{L}^T l - m\boldsymbol{F} + \frac{\partial\left\{\left[\left(s_0 \int_V \frac{B^T QB}{\bar{\dot{e}}}\right)\dot{\boldsymbol{u}}\right]\right\}}{\partial \dot{\boldsymbol{u}}} D\dot{\boldsymbol{u}} = 0 \qquad \text{...(3.64b)}$$

or,

$$\frac{\partial\left\{\left[\left(s_0 \int_V \frac{B^T QB}{\bar{\dot{e}}}\right)\dot{\boldsymbol{u}}\right]\right\}}{\partial \dot{\boldsymbol{u}}} = \left(s_0 \int_V \frac{B^T QB}{\bar{\dot{e}}}\right) - \left(s_0 \int_V \frac{B^T QB\dot{\boldsymbol{u}}_e}{\bar{\dot{e}}^2}\right) \bullet \frac{\partial \bar{\dot{e}}}{\partial \dot{\boldsymbol{u}}_e} \qquad \text{...(3.65)}$$

$$= \int_V s_0 \left(\frac{B^T QB}{\bar{\dot{e}}} - \frac{B^T QB\dot{\boldsymbol{u}}_e \dot{\boldsymbol{u}}_e B^T QB}{\bar{\dot{e}}^3}\right) dV$$

Thus,

$$\frac{\partial \bar{\dot{e}}}{\partial \dot{\boldsymbol{u}}_e} = \frac{\partial \sqrt{(B\dot{\boldsymbol{u}}_e)^T QB\dot{\boldsymbol{u}}_e}}{\partial \dot{\boldsymbol{u}}_e} = \frac{1}{\bar{\dot{e}}} \dot{\boldsymbol{u}}_e{}^T B^T QB \qquad \text{...(3.66)}$$

Similarly,

$$L\dot{\boldsymbol{u}} + LD\dot{\boldsymbol{u}} = 0 \qquad \text{...(3.67)}$$

$$\boldsymbol{F}^T \dot{\boldsymbol{u}} + \boldsymbol{F}^T D\dot{\boldsymbol{u}} = 1 \qquad \text{...(3.68)}$$

Finally, the following equations are solved for $D\dot{\boldsymbol{u}}$, l and m.

$$\int_V s_0 \left(\frac{B^T QB}{\bar{\dot{e}}} - \frac{B^T QB\dot{\boldsymbol{u}}_e \dot{\boldsymbol{u}}_e B^T QB}{\bar{\dot{e}}^3}\right) dV\, D\dot{\boldsymbol{u}} + \boldsymbol{L}^T l - m\boldsymbol{F} = -\left(\int_V s_0 \frac{B^T QB}{\bar{\dot{e}}}\right)\dot{\boldsymbol{u}} \qquad \text{(3.69a)}$$

$$LD\dot{\boldsymbol{u}} = -L\dot{\boldsymbol{u}} \qquad \text{…(3.69b)}$$

$$\boldsymbol{F}^T D\dot{\boldsymbol{u}} = 1 - \boldsymbol{F}^T \dot{\boldsymbol{u}} \qquad \text{…(3.69c)}$$

3.3 FORMULATION OF REINFORCED SOIL SYSTEM

3.3.1 Axial Force: *"no-length change" Condition*

As mentioned in the introduction, the concept we assume is that the length between arbitrary soil element nodes touching the reinforcement material does not change in the soil mass at failure. In other words, the soil elements flow with the reinforcing material keeping the length constant in the soil mass at the limiting equilibrium state. Under this condition the reinforcing material restrains the flow of soil elements (i.e. plastic flow) keeping the nodal distance constant. It should be noted that the real reinforcing steel bars or geotextiles never appear in this computational work.

Let us incorporate this reinforced mechanism in RPFEM. Referring Fig. 3.6, let A and B are soil element nodes touching the reinforcing material and having positions vectors $\boldsymbol{X}_1$ and $\boldsymbol{X}_2$, respectively. Now, consider $\boldsymbol{l}$ $(=\boldsymbol{X}_2-\boldsymbol{X}_1)$ is displaced to $\boldsymbol{l}+\Delta\boldsymbol{l}$ in arbitrary small time dt at failure. Meanwhile, it is assumed that the relative position between A and B remains constant during plastic flow. Mathematically,

$$|\boldsymbol{l}| = |\boldsymbol{l}+\Delta\boldsymbol{l}| \qquad ...(3.70)$$

Therefore,

$$(\boldsymbol{l}+\Delta\boldsymbol{l})^T(\boldsymbol{l}+\Delta\boldsymbol{l}) - \boldsymbol{l}^T\boldsymbol{l} = 0 \qquad ...(3.71)$$

$$\boldsymbol{l}^T\boldsymbol{l} + \boldsymbol{l}^T\Delta\boldsymbol{l} + \Delta\boldsymbol{l}^T\boldsymbol{l} + \Delta\boldsymbol{l}^T\Delta\boldsymbol{l} - \boldsymbol{l}^T\boldsymbol{l} = \boldsymbol{0} \qquad ...(3.72)$$

where T implies the transpose of vector (or Matrix)

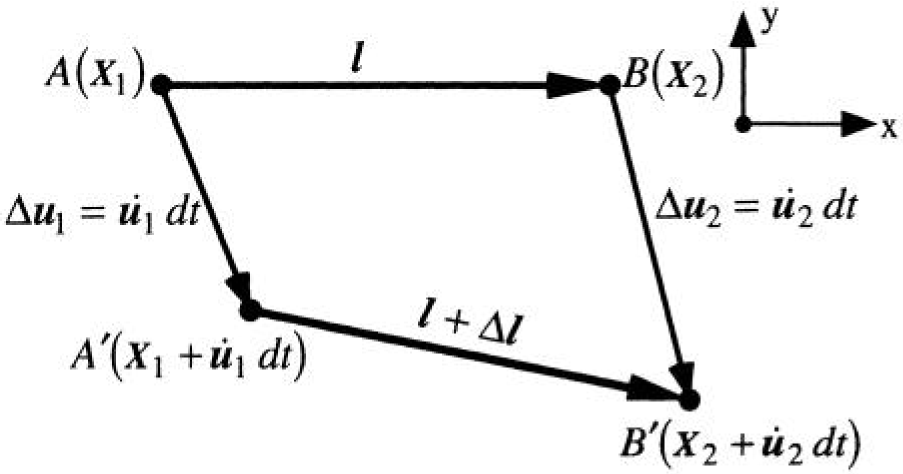

Figure 3.6 Concept of "*no-length change*" condition at limiting equilibrium state.

After some mathematical manipulations, i.e. neglecting higher order terms, Eq.(3.72) is reduced to the following form,

$$\boldsymbol{l}^T D\,\boldsymbol{l} = 0 \qquad ...(3.73)$$

Referring Fig. 3.6, the vector $D\,\boldsymbol{l}$ can be expanded as follows:

$$\boldsymbol{l} + D\boldsymbol{l} = \boldsymbol{X}_2 + D\boldsymbol{u}_2 - (\boldsymbol{X}_1 + D\boldsymbol{u}_1) \qquad ...(3.74)$$

or,

$$\boldsymbol{l} + D\boldsymbol{l} = \boldsymbol{X}_2 - \boldsymbol{X}_1 + (D\boldsymbol{u}_2 - D\boldsymbol{u}_1) \qquad ...(3.75)$$

Since $\boldsymbol{l} = (\boldsymbol{X}_2 - \boldsymbol{X}_1)$ in Fig. 3.6, then vector $D\,\boldsymbol{l}$ reduced to the following form:

$$D\boldsymbol{l} = D\boldsymbol{u}_2 - D\boldsymbol{u}_1 = \dot{\boldsymbol{u}}_2 dt - \dot{\boldsymbol{u}}_1 dt \; D\boldsymbol{l} = D\boldsymbol{u}_2 - D\dot{\boldsymbol{u}}_1 = \dot{\boldsymbol{u}}_2 dt - \dot{\boldsymbol{u}}_1 dt \qquad ...(3.76)$$

where $D\,\dot{\boldsymbol{u}}_1$ and $D\,\dot{\boldsymbol{u}}_2$ are the displacements of A and B in arbitrary time dt and $\dot{\boldsymbol{u}}_1$ and $\dot{\boldsymbol{u}}_2$ are the velocities corresponding to A and B respectively. After eliminating the scalar quantity dt the equation reduces to

$$(\boldsymbol{X}_2 - \boldsymbol{X}_1)^T (\dot{\boldsymbol{u}}_2 - \dot{\boldsymbol{u}}_1) = 0 \qquad ...(3.77)$$

Since $\boldsymbol{X}_1 \neq \boldsymbol{X}_2$ the velocities obtained by employing the constrained condition of no length change should satisfy either of the following relations:

$$\text{Either} \quad \dot{\boldsymbol{u}}_1 = \dot{\boldsymbol{u}}_2 \quad \text{or} \quad (\boldsymbol{X}_2 - \boldsymbol{X}_1) \perp (\dot{\boldsymbol{u}}_2 - \dot{\boldsymbol{u}}_1) \qquad ...(3.78)$$

Now, expanding the position vectors and velocity vectors

$$\boldsymbol{X}_1 = \begin{pmatrix} x_1 \\ y_1 \end{pmatrix} \quad \boldsymbol{X}_2 = \begin{pmatrix} x_2 \\ y_2 \end{pmatrix} \quad \dot{\boldsymbol{u}}_1 = \begin{pmatrix} \dot{u}_{x1} \\ \dot{u}_{y1} \end{pmatrix} \quad \dot{\boldsymbol{u}}_2 = \begin{pmatrix} \dot{u}_{x2} \\ \dot{u}_{y2} \end{pmatrix} \qquad ...(3.79)$$

and incorporating these terms in Eq. (3.77)

$$(x_2 - x_1)(\dot{u}_{x2} - \dot{u}_{x1}) + (y_2 - y_1)(\dot{u}_{y2} - \dot{u}_{y1}) = 0 \qquad ...(3.80)$$

The equation Eq.(3.80) can be presented in the following matrix form:

$$\big((x_2 - x_1) \quad (y_2 - y_1) \quad -(x_2 - x_1) \quad -(y_2 - y_1)\big) \begin{Bmatrix} \dot{u}_{x1} \\ \dot{u}_{y1} \\ \dot{u}_{x2} \\ \dot{u}_{y2} \end{Bmatrix} = 0 \qquad ...(3.81)$$

Since Eq. (3.77)(or Eq. (3.80)) is a linear algebraic equation, we can easily incorporate this in the RPFEM/LEFEM as a constrained condition. This constrained condition represents a basic reinforcing element and it can be extended to other continuous reinforcing members by discretizing them into finite numbers of such basic discrete elements. Such procedure is illustrated in the next paragraphs.

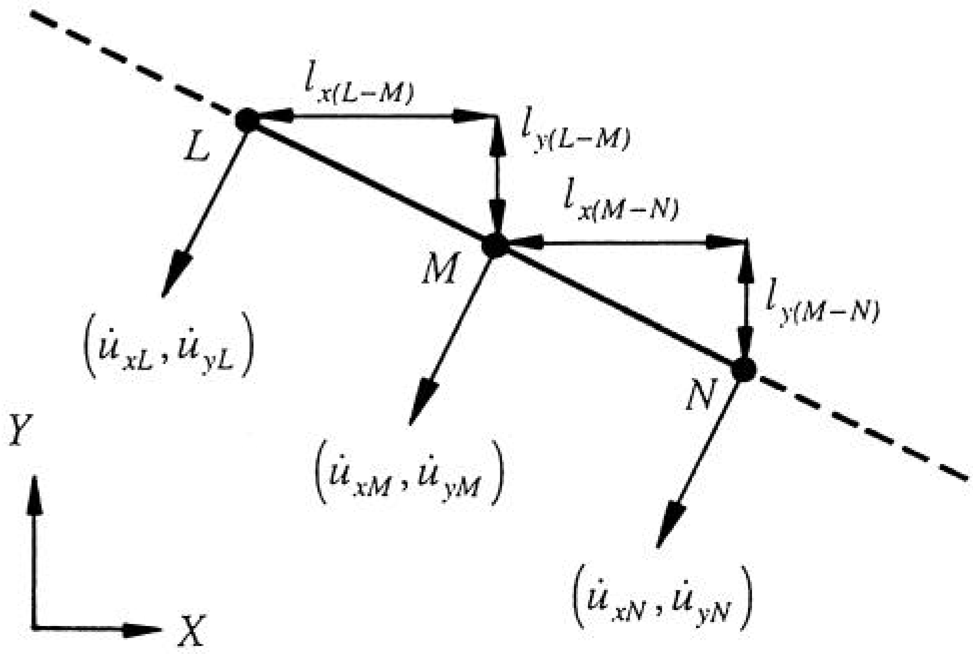

Figure 3.7 Graphical explanation of length components for a typical reinforcing element under axial tension.

Consider three nodes L, M and N are constrained by the reinforcing system as shown in Figs. 3.7 and 3.8. Then, the x and y components of the length vector between nodes L and M are:

$$l_{x(L-M)} = x_2 - x_1 \quad \text{and} \quad l_{y(L-M)} = y_2 - y_1 \qquad ...(3.82)$$

Thus, replacing the Cartesian components by absolute length components, the constrained condition corresponding to nodes L & M can be simplified to:

$$\begin{pmatrix} l_{x(M-N)} & l_{y(M-N)} & -l_{x(M-N)} & -l_{y(M-N)} \end{pmatrix} \begin{Bmatrix} \dot{u}_{xM} \\ \dot{u}_{yM} \\ \dot{u}_{xN} \\ \dot{u}_{yN} \end{Bmatrix} = 0 \qquad ...(3.83)$$

and similarly for nodes M & N:

$$\begin{pmatrix} l_{x(M-N)} & l_{y(M-N)} & -l_{x(M-N)} & -l_{y(M-N)} \end{pmatrix} \begin{Bmatrix} \dot{u}_{xM} \\ \dot{u}_{yM} \\ \dot{u}_{xN} \\ \dot{u}_{yN} \end{Bmatrix} = 0 \qquad ...(3.84)$$

Such equations corresponding to all reinforcing element nodes can be finally assembled into the following single equation:

$$C_t \ \dot{\boldsymbol{u}} = 0 \qquad ...(3.85)$$

which is equivalent to Eq. (3.77) or Eq. (3.80). The matrix C_t produces a set of equations similar to Eq.(3.80) when all nodal velocity vectors are multiplied by C_t . Thus, these equations represent the "*constrained conditions*" for the respective reinforcing element nodes.

The assembled positions of the aforementioned reinforcing element nodes is illustrated in the following expanded form of matrix C_t .

$$(C_t) = \begin{pmatrix} & .... & .... & .... & .... & .... & .... & \\ 0 & l_{x(L-M)} & l_{y(L-M)} & -l_{x(L-M)} & -l_{y(L-M)} & 0 & 0 & 0 \\ 0 & 0 & 0 & l_{x(M-N)} & l_{y(M-N)} & -l_{y(M-N)} & -l_{y(M-N)} & 0 \\ & & .... & .... & .... & .... & .... & \end{pmatrix} .(3.86)$$

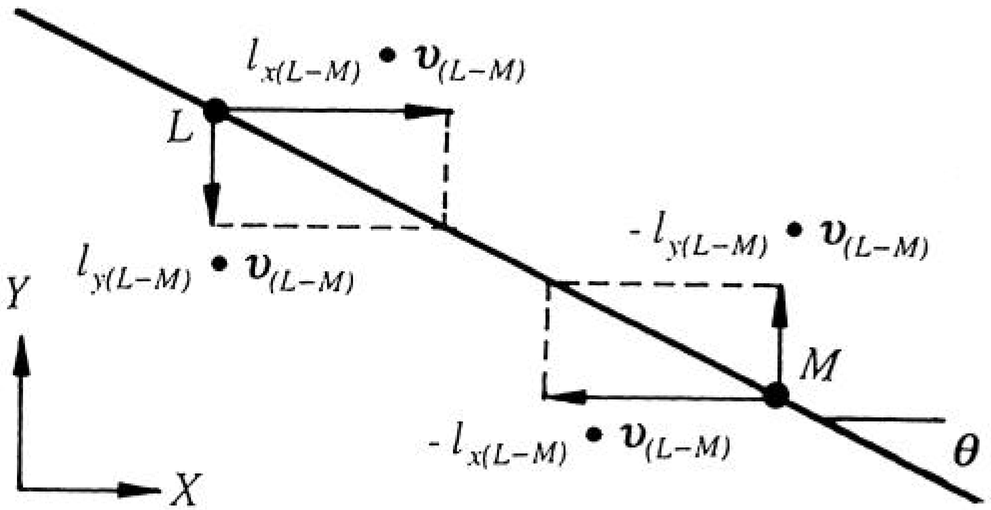

Figure 3.8 Graphical explanation of Lagrange multipliers corresponding to the linear constraint condition of "*no-length change*" condition.

3.3.2 Shear Force/Bending Moment: "*no-bending*" *Condition*

In this study, it is assumed that the soil elements along a reinforcing material that is practically rigid in bending (e.g. facing panel, shotcrete, sheet pile, etc.) do not change their relative positions during the plastic flow of soil elements at limit state.

In Figure 3.9, the three points A, B and C make a straight line and maintain the straight line throughout the limiting equilibrium state of soil mass. The no-bending condition, here, is formulated along with the no-length change condition imposed on the corresponding reinforced soil element nodes. Mathematically, the no-length change condition for a reinforcement means the displacement components parallel to the reinforcement are assumed to be constant as follows:

$$\left|D\boldsymbol{u}_i\right| cos\boldsymbol{b}_i = \text{constant} \qquad ...(3.87)$$

or, in velocity terms

$$\left|\dot{\boldsymbol{u}}_i\right| cos\boldsymbol{b}_i \; dt = \text{constant} \qquad ...(3.88)$$

where dt is a scalar quantity and thus satisfies. $\left|\dot{\boldsymbol{u}}_i\right| = \left|\boldsymbol{u}_i\right| dt$ Then, referring the Figs.3.9~3.11,

$$\left|\dot{\boldsymbol{u}}_1\right| cos\boldsymbol{b}_1 = \left|\dot{\boldsymbol{u}}_2\right| cos\boldsymbol{b}_2 = \left|\dot{\boldsymbol{u}}_3\right| cos\boldsymbol{b}_3 \qquad ...(3.89)$$

In order to formulate the no-bending condition under the no-length change assumption (Eq. 3.87), the following condition is introduced in this study:

$$\left|l_1\right| : \left(\left|\dot{\boldsymbol{u}}_2\right| sinb_2 - \left|\dot{\boldsymbol{u}}_1\right| sinb_1\right) = \left|l_2\right| : \left(\left|\dot{\boldsymbol{u}}_3\right| sinb_3 - \left|\dot{\boldsymbol{u}}_2\right| sinb_2\right) \qquad ...(3.90)$$

which yields,

$$-\left|l_2\right|\left|\dot{\boldsymbol{u}}_1\right| sinb_1 + \left(\left|l_1\right| + \left|l_2\right|\right)\left|\dot{\boldsymbol{u}}_2\right| sinb_2 - \left|l_1\right|\left|\dot{\boldsymbol{u}}_3\right| sinb_3 = 0 \qquad ...(3.91)$$

The first term of Eq. (3.91) is simplified as follows:

$$\begin{aligned} |l_2|\,|\dot{u}_1|\sin\beta_1 &= |l_2|AD = |l_2|A'E = |l_2|(A'E' - E'E) = |l_2|(A'E' - FF') \\ &= |l_2|\,|\dot{u}_1|sin(\alpha+\beta_1)cos\alpha - |l_2|\,|\dot{u}_1|cos(\alpha+\beta_1)sin\alpha \\ &= |l_2|cos\alpha\,|\dot{u}_1|sin(\alpha+\beta_1) - |l_2|sin\alpha\,|\dot{u}_1|cos(\alpha+\beta_1) \\ &= l_{2x}\,\dot{u}_{1y} - l_{2y}\,\dot{u}_{1x} \end{aligned} \qquad ...(3.92)$$

in which the subscripts x and y express the Cartesian components of vectors. Geometrically various components of velocity $\dot{\boldsymbol{u}}_1$ are illustrated in Fig.3.11. The length components for a typical bending element are illustrated in Fig. 3.11.

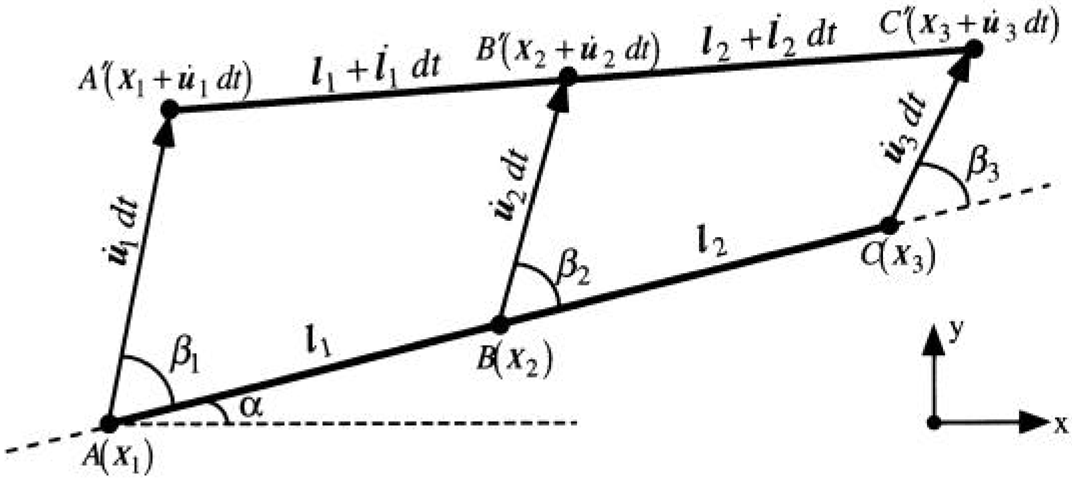

Figure 3.9 Concept of "*no-bending*" condition at limiting equilibrium state

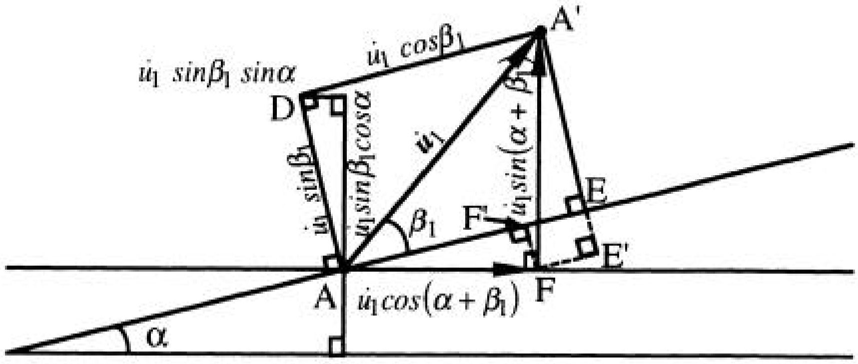

Figure 3.10 Graphical details of length components for a typical velocity vector.

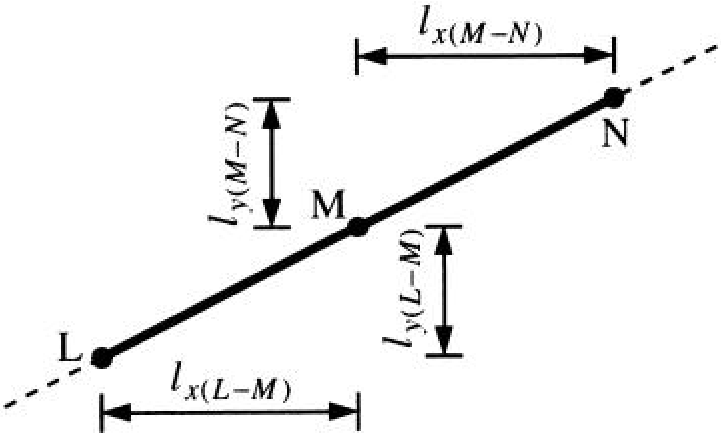

Figure 3.11 Graphical explanation of length components for a typical bending element.

Meanwhile, such simplified forms (e.g. Eq.3.92) can be obtained for the last two terms in Eq. (3.91) following the similar procedure. Thus, the simplified forms corresponding to these two terms are as follows:

$$(|l_1|+|l_2|)|\dot{u}_2|\sin\beta_2 = (l_{1x}+l_{2x})\dot{u}_{2y} - (l_{1y}+l_{2y})\dot{u}_{2x} \qquad ..(3.93)$$

and

$$|l_3|\,|\dot{u}_3|\sin\beta_3 = l_{1x}\,\dot{u}_{3y} - l_{1y}\,\dot{u}_{3x} \qquad ..(3.94)$$

Thus, the equation, Eq.(3.91) can be expressed in the following simplified form:

$$-(l_{2x}\,\dot{u}_{1y} - l_{2y}\,\dot{u}_{1x}) + (l_{1x}+l_{2x})\dot{u}_{2y} - (l_{1y}+l_{2y})\dot{u}_{2x} - (l_{1x}\,\dot{u}_{3y} - l_{1y}\,\dot{u}_{3x}) = 0 \qquad ..(3.95)$$

or, $$l_{2y}\,\dot{u}_{1x} - l_{2x}\,\dot{u}_{1y} - (l_{1y}+l_{2y})\dot{u}_{2x} + (l_{1x}+l_{2x})\dot{u}_{2y} + l_{1y}\,\dot{u}_{3x} - l_{1x}\,\dot{u}_{3y} = 0 \qquad ...(3.96)$$

Finally, the "*no bending condition*" (i.e. Eq.3.91 or Eq.3.96) can be expressed in the matrix form as a linear constrained condition on the velocity corresponding to three reinforced points as shown in Fig.3.9.

$$\left(l_{2y}, -l_{2x}, -(l_{1y}+l_{2y}), (l_{1x}+l_{2x}), l_{1y}, -l_{1x}\right)\cdot\left(\dot{u}_{1x}, \dot{u}_{1y}, \dot{u}_{2x}, \dot{u}_{2y}, \dot{u}_{3x}, \dot{u}_{3y}\right)^T = 0 \qquad ...(3.97)$$

This equation can be also expanded to assemble all the nodal velocity vectors using the matrix C_b similarly as in the "*no length change condition*", *see* Eq. (3.86), i.e. the matrix, C_t.

$$C_b\ \dot{\boldsymbol{u}} = 0 \qquad ...(3.98)$$

where C_b in the case shown in Fig.3.11 can be expressed as follows:

$$C_b = \begin{pmatrix} \cdots & \cdots & \cdots & \cdots & \cdots & \cdots & \cdots & \cdots \\ \cdots & l_{y(M-N)} & -l_{x(M-N)} & \begin{matrix}-(l_{y(L-M)} \\ +l_{y(M-N)})\end{matrix} & \begin{matrix}-(l_{x(L-M)} \\ +l_{x(M-N)})\end{matrix} & l_{y(L-M)} & -l_{x(L-M)} & \cdots \\ \cdots & \cdots & \cdots & \cdots & \cdots & \cdots & \cdots & \cdots \end{pmatrix} \qquad ...(3.99)$$

Points L, M and N form a basic (unit) reinforcing system for all the reinforcement under bending.

3.4 INCORPORATIONS OF CONSTRAINT CONDITIONS

3.4.1 Incorporating into the RPFEM

On the basis of the upper bound theorem on plasticity, the rigid plastic finite element method (RPFEM) is obtained through minimizing the rate of internal plastic energy dissipation with respect to the kinematically admissible velocity field under several linear constraint conditions (Tamura et al. 1984). In this study, these are summarized as follows: (1) soils are assumed to exhibit no rate of volume change at the limit state like the plastic flow of Mises material. (2) Loading is made through a velocity/displacement boundary like through a rigid footing. In addition to these constraints, (3) "*no length change*" and (4) "*no-bending*" conditions are imposed upon the velocity along reinforcements. Mathematically, these are all linear constraint conditions.

The formulation is employed by introducing the Lagrange multipliers l, m, n and x to solve the minimization problem under constraint conditions. Finally, the following function is minimized.

$$\varphi(\dot{u}, \boldsymbol{\lambda}, \boldsymbol{\mu}, \boldsymbol{\nu}, \boldsymbol{\xi}) = \int_V D(\dot{u})dV + \boldsymbol{\lambda}^T(L\dot{u} - \mathbf{0}) + \boldsymbol{\mu}(C\dot{u} - \boldsymbol{a}) + \boldsymbol{\nu}^T(C_t\dot{u} - \mathbf{0}) + \boldsymbol{\xi}^T(C_b\dot{u} - \mathbf{0}) \quad \text{...(3.100)}$$

in which $\boldsymbol{D}$ is the rate of internal plastic energy dissipation. L is the matrix defined such as $L\dot{\boldsymbol{u}} = \dot{\boldsymbol{v}}$ where $\dot{\boldsymbol{v}}$ is the rate of volume changes in all elements. Therefore the first constraint condition, $L\dot{\boldsymbol{u}}=0$ indicates that no rates of volume change occur in all the elements at the limit state. The vector $\boldsymbol{a}$ is a prescribed vector only at the displacement boundary and the matrix C retrieves the velocity vector at the displacement boundary when all nodal velocity vectors, $\dot{\boldsymbol{u}}$, are multiplied by C. Therefore, the second constraint condition, $C\dot{\boldsymbol{u}}=\boldsymbol{a}$ defines the provisional norms of velocity vector beneath the rigid loading plate. The third constraint condition, $C_t\dot{\boldsymbol{u}}=\mathbf{0}$ indicates the "no length change condition", *see* Eq. (3.88), while the forth one, $C_b\dot{\boldsymbol{u}}=\mathbf{0}$, indicates the "no-bending condition", *see* Eq. (3.93). As the rate of internal plastic energy dissipation, $D(\dot{\boldsymbol{u}})$ is the convex function of $\dot{\boldsymbol{u}}$, a local stationary condition of J gives the global minimum of J. Then taking the derivative of function, J, one has the following equilibrium equation of forces at limit state and accompanied constraint conditions.

$$\int_V B^T \boldsymbol{s}\, dV + L^T l + C^T m + C_t{}^T n + C_b{}^T x = \mathbf{0} \quad \text{...(3.101)}$$

$$L\dot{\boldsymbol{u}} = 0 \quad \text{...(3.102)}$$

$$C\dot{\boldsymbol{u}} = \boldsymbol{a} \quad \text{...(3.103)}$$

$$C_t\dot{\boldsymbol{u}} = \mathbf{0} \quad \text{...(3.104)}$$

$$C_b\dot{\boldsymbol{u}} = \mathbf{0} \quad \text{...(3.105)}$$

in which $\boldsymbol{s}$ denotes deviator stress vector while Lagrange multipliers l and m are interpreted as the indeterminate isotropic stress and the contact pressure at the prescribed displacement boundary, respectively (Tamura et al., 1984). Interpretation of the other two newly introduced

Lagrange multipliers (n and x) are mentioned in the following section.

3.4.2 Interpretation of the Lagrange Multipliers

The Lagrange multiplier n is interpreted as the unit nodal forces acting on constrained nodes along the reinforcement direction, while x is also interpreted as the unit nodal forces acting on constrained nodes but along the perpendicular direction to the reinforcement. In other words, the forces calculated as x appear at the reinforced system that remains straight, e. g. points A, B and C in Fig. 3.9, to resist the bending moment in the reinforced system. For instance, the

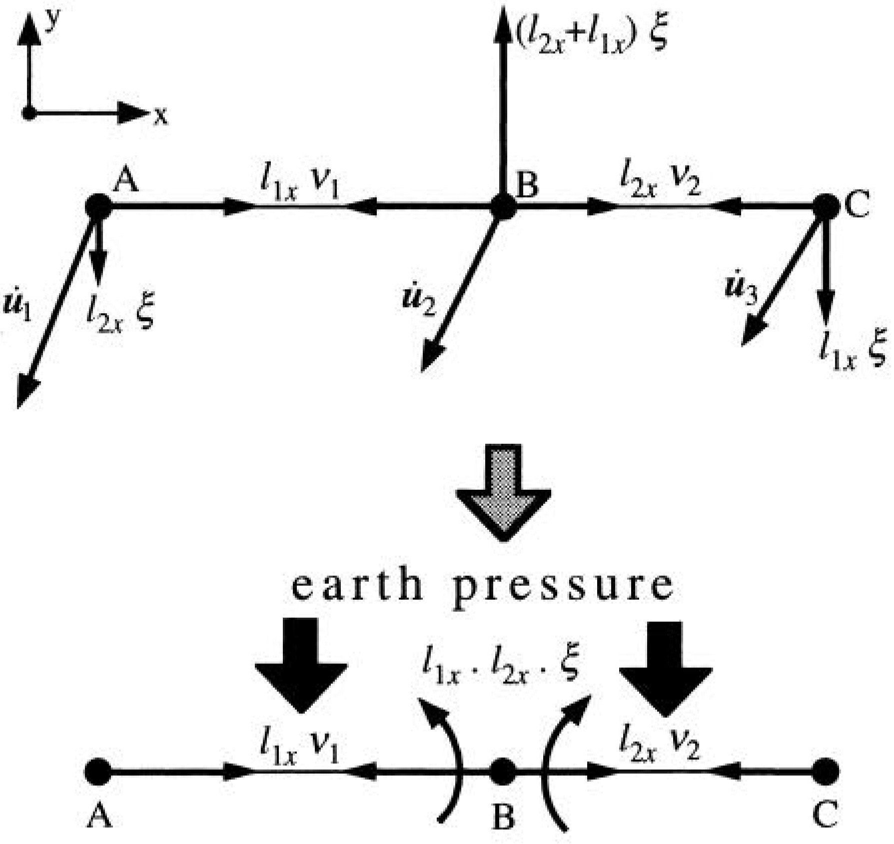

Figure 3.12 Graphical explanation of Lagrange multipliers corresponding to the linear constraint condition of "*no-bending*" conditions.

forces calculated as n and x in the horizontal reinforcement as shown in Figs. 3.8 and 3.12 are described. The fourth term in Eq.(3.101), $C_t{}^T n$, can be rewritten by the x, y component of the points A, B and C as follows:

$$C_t{}^T n = \left(l_{1x} n_1,\ 0,\ l_{2y},\ -l_{1x} n_1 + l_{2x} n_2,\ 0,\ -l_{2x} n_2,\ 0\right)^T \qquad ...(3.106)$$

These forces act to resist extension of the distance between the constrained nodes along the reinforcement during failure. The fifth term in Eq. (3.101), $C_b{}^T x$ can be rewritten similarly to Eq. (3.104) as follows:

$$C_t{}^T x = \left(0,\ -l_{2x} x,\ 0,\ (l_{2x} + l_{1x}) x,\ 0,\ -l_{1x} x\right)^T \qquad (3.107)$$

These forces, which are interpreted as shear forces, resist bending of the straight line due to the earth pressure during failure. Furthermore the resistant to bending moment occur in the reinforced system is calculated as follow:

$$l_{1x} \cdot l_{2x} \cdot x \qquad (3.108)$$

A complete reinforced system that is designed to resist developed bending moment in the system can be modeled by having such bending elements in series where neighboring three nodes can overlap each other in series. The resistant to bending moments can be superimposed.

3.4.3 Incorporating into the LEFEM

Strain-displacement compatibility:

The strain tensor, e_{ij}, can be derived from the displacements u_i by means of the following compatibility relation assuming small strain:

$$e_{ij} = \frac{1}{2}\left(u_{i,j} + u_{j,i}\right) \quad in \ \ V \qquad ...(3.109)$$

where a comma preceding a subscript i denotes partial differentiation with respect to the coordinate x_i.

Boundary condition The displacements satisfy the boundary conditions on S_u

$$u_i = u_{io} \qquad ...(3.110)$$

Equilibrium equation: Neglecting the geometry change due to the deformation in deriving the equations of equilibrium, it is immaterial whether the symmetric stress tensor σ_{ij} is referred to the undeformed or the deformed state. Denoting the body forces per unit volume by X_i and the surface tractions by T_i, the equations of equilibrium in the interior of the body are

$$s_{ij,j} + X_i = 0 \quad ...(3.111)$$

and the boundary conditions on the surface are

$$s_{ij}.n_j = T_i \quad ...(3.112)$$

where n_i is the unit outward normal vector to the surface and the summation convention for repeated subscripts has been employed .

The conditions of equilibrium may be compressed into a single equation

$$\int_V s_{ij}\, e_{ij} dV = \int_{S_s} T_i\, \delta u_i \; dS + \int_V X_i \delta u_i \; dV \quad ...(3.113)$$

holding for any stress distribution s_{ij} in equilibrium with the external loads X_i, T_i and for any displacement field u_i with its corresponding strain distribution e_{ij}. This equilibrium equation is the basic tool in the derivation of linear elastic finite element formulations.

***General stress-strain relations*:**

The tensor of elastic coefficient has the properties of symmetry

$$\sigma D = \varepsilon \quad ...(3.114)$$

or,

$$\sigma = D^{-1} \varepsilon \quad ...(3.115)$$

The elastic strain energy per unit volume

$$\Pi(\boldsymbol{u}, n, x) = \int_V \frac{1}{2} s^T e \, dV \quad ...(3.116)$$

unless all stresses are zero and the inversion of the relations Eq.(3.114) is also unique.

The initial tangential load-deformation curve of the reinforced soil structure is estimated in this study approximately by using the linear elastic theory (E,υ).

The potential energy is minimized introducing constraint conditions on the deformation field, which is almost the same as that in minimizing the rate of internal plastic dissipation corresponding to the aforementioned RPFEM. The energy function in Eq.(3.116) is modified to satisfy the constraint conditions, as follows:

$$F(\boldsymbol{u}, n, x) = \int_V \frac{1}{2} s^T e \, dV + n^T (C_t \, \boldsymbol{u} - \boldsymbol{0}) + x^T (C_b \, \boldsymbol{u} - \boldsymbol{0}) - F \, \boldsymbol{u}^T \quad ...(3.117)$$

Minimization of this energy function yields a set of simultaneous equations with constraint conditions is as follows:

$$\int_V B^T DB \ dV \, \boldsymbol{u} + C_t^T \, n + C_b^T \, x - F = \mathbf{0} \qquad ...(3.118)$$

$$C_t \boldsymbol{u} = \mathbf{0} \qquad ...(3.119)$$

$$C_b \, \boldsymbol{u} = \mathbf{0} \qquad ...(3.120)$$

in which the matrix D defines the constitutive relationship of the linear elastic material based on the Hook's law. These Lagrange multipliers can be interpreted similarly as in the RPFEM.

3.5 SUMMARY AND CONCLUDING REMARKS

A simplified tool for the analysis and design of complex reinforced soil structures is formulated based on plasticity theories at the limit state of soil mass. This method presents a new concept of computation of bearing capacity/safety factor, distribution of axial and shear (/bending) forces as well as velocity vectors and the stress distribution in the reinforced soil structures is simultaneously formulated. The reinforced effect is coupled in the conventional rigid plastic finite element method by introducing a set of linear constraint conditions of '*ho length change*" and "*no-bending*" upon the soil element nodes corresponding to reinforcement at the limit equilibrium state.

The conclusions drawn from the present chapter on formulation of the reinforced soil system are as follows:

1. The mechanism of the reinforcement and facing can be modeled by introducing the two new linear constraint conditions, "*no-length change*" and "*no-bending*", in the two energy functions: stored energy function in linear elastic problems and the plastic energy dissipation function in limit state problems.
2. Lagrange multipliers corresponding to these constraint conditions represent the axial force and shear force (/bending moment) in the reinforcing material per unit length, respectively.
3. The effect of rigid panel facing in bending can also be formulated using the same concept. It can be explained with the bending moment developed in the facing.
4. Frictional material can be modeled as an assembly of inhomogeneous Mises material whose shear strength depends on the confining pressure.